Physics Letters B 694 (2011) 289–293

Contents lists available at ScienceDirect

Physics Letters B

www.elsevier.com/locate/physletb

Ruling out the Modified Chaplygin Gas cosmologies

J.C. Fabris [a,*], H.E.S. Velten [a], C. Ogouyandjou [b], J. Tossa [b]

[a] Departamento de Física, Universidade Federal do Espírito Santo, CEP 29060-900 Vitória, Espírito Santo, Brazil
[b] Institut des Mathématiques et des Sciences Physiques - IMSP, B.P. 613, Porto Novo, Benin

ARTICLE INFO

Article history:
Received 6 July 2010
Received in revised form 10 September 2010
Accepted 13 October 2010
Available online 16 October 2010
Editor: S. Dodelson

Keywords:
Dark energy
Unified models
Cosmology

ABSTRACT

The Modified Chaplygin Gas (MCG) model belongs to the class of a unified models of dark energy (DE) and dark matter (DM). It is characterized by an equation of state (EoS) $p_c = B\rho - A/\rho^\alpha$, where the case $B = 0$ corresponds to the Generalized Chaplygin Gas (GCG) model. Using a perturbative analysis and power spectrum observational data we show that the MCG model is not a successful candidate for the cosmic medium unless $B = 0$. In this case, it reduces to the usual GCG model.

1. Introduction

The cross of different observational results at cosmological level indicates that besides the usual expected contents of the cosmic budget, like baryons and radiation, there is a dark sector, with two components, dark matter and dark energy. In principle, dark matter is present in local structures like galaxies and cluster of galaxies, suffering consequently the process of gravitational collapse. In this sense, dark matter behaves much as like ordinary matter. However, it does emit any kind of electromagnetic radiation. Dark energy, on the other hand, seems to remain a smooth, not clustered, component, driving the accelerated expansion of the universe. This property requires a negative pressure. Many different models have been evoked to describe this dark sector of the energy content of the universe, going from the inclusion of exotic components in the context of general relativity theory to modifications of the gravitational theory itself, passing by other possibilities as the breakdown of the homogeneity condition. For a recent review, see Ref. [1].

A very appealing proposal to describe the dark sector are the so-called unified models. The prototype of such model is the Chaplygin gas [2–4]. In the unified model dark matter and dark energy are described by a single fluid, which behaves as ordinary matter in the past, and as a cosmological constant term in the future. In this sense, it interpolates the different periods of evolution of the universe, including the present stage of accelerated expansion. The Chaplygin gas model leads to very good results when confronted with the observational data of supernova type Ia [5]. Concerning the matter power spectrum data, the statistic analysis leads to results competitive with the ΛCDM model, but the unified (called quartessence) scenario must be imposed from the beginning [6,7]. This means that the only pressureless component admitted is the usual baryonic one, otherwise there is a conflict between the constraints obtained from the matter power spectrum and the supernova tests.

Many variations of the Chaplygin gas model have been proposed in the literature. One of them is the Modified Chaplygin Gas (MCG) Model. The equation of state of the MCGM is

$$p_c = B\rho - A\rho^{-\alpha}, \tag{1}$$

where B, A and α are constants. When $B = 0$ we recover the Generalized Chaplygin Gas (GCG) Model, and if in addition $\alpha = 1$ we have the original Chaplygin gas model. The dynamics of the MCG model has been studied in Ref. [8], while a dynamical system analysis has been made in Ref. [9]. The evolution of the temperature function has been considered in Ref. [10]. Some background constraints were established in Refs. [11] and [12]. The analysis of the spherical collapse was made in Ref. [13], while a perturbative study, looking for some general features of the model, was carried out in Ref. [14]. In all these studies the viability of the model was concluded, but no one of them has exploited the observational data concerning the perturbative behavior of the model.

* Corresponding author.
E-mail addresses: fabris@pq.cnpq.br (J.C. Fabris), velten@cce.ufes.br (H.E.S. Velten), ogouyandjou@imsp-uac.org (C. Ogouyandjou), joel.tossa@imsp-uac.org (J. Tossa).

0370-2693/$ – see front matter
doi:10.1016/j.physletb.2010.10.022

Our intention here is to test the MCG model against the power spectrum observational data. For the background tests, as those analyzed in Refs. [11,12], the MCG reveals to lead to competitive scenarios compared with the ΛCDM and the GCG models (to give just some examples). However, the constraints coming from the power spectrum data are, in general, much more crucial since it tests not only the background framework, but also the perturbative behavior of the model. Many general constraints can be established on the parameters of the EoS (1) even not considering perturbations. For example, in the past the equation of state (1) implies, when α is positive (a requirement necessary in a perturbative analysis in order to preserve a positive sound speed) that

$$\rho_c(a \approx 0) = \frac{cte}{a^{3(1+B)}}. \tag{2}$$

In order not to spoil the usual primordial scenario of the standard model (in special nucleosynthesis), B must be smaller than 1/3, which may include negative values. On the other hand, as we will show below, the requirement that the sound speed of the MCG must be positive implies essentially that $B > 0$. Hence, the admissible values of the parameter B seems to be around $0 < B < 1/3$. These considerations will be strengthened through the power spectrum analysis to be made later in this Letter: the matter power spectrum data can be fitted only if $|B| < 10^{-6}$. Hence, essentially the only configuration possible is that corresponding to the generalized Chaplygin gas, with perhaps some possible very small deviations from it. In this sense, we can consider that the MCG model is ruled out when confronted with the power spectrum observational data.

In next section we set out the general equations of the MCG model at background and perturbative levels. In Section 3 we perform a numerical analysis comparing the theoretical results with the matter power spectrum observational data. In Section 4 we present our conclusions.

2. Basic set of equations

Our starting point are Einstein's equations coupled to a pressureless fluid, radiation and to the MCG fluid. They read,

$$R_{\mu\nu} = 8\pi G\left\{T^m_{\mu\nu} - \frac{1}{2}g_{\mu\nu}T^m\right\} + 8\pi G\left\{T^r_{\mu\nu} - \frac{1}{2}g_{\mu\nu}T^r\right\} + 8\pi G\left\{T^c_{\mu\nu} - \frac{1}{2}g_{\mu\nu}T^c\right\},$$

$$T^{\mu\nu}_{m;\mu} = 0, \quad T^{\mu\nu}_{c;\mu} = 0, \quad T^{\mu\nu}_{r;\mu} = 0.$$

The superscripts (subscripts) m, r and c stand for "matter", "radiation" and "Chaplygin". We assume a perfect fluid structure for the cosmic medium as a whole and also for each of the components,

$$T^{\mu\nu}_A = (\rho_A + p_A)u^\mu_A u^\nu_A - p_A g^{\mu\nu}, \qquad A = m, c, r. \tag{3}$$

Note that for "matter" component we understand a pressureless fluid that, in principle, may include baryons and dark matter. This questions will be discussed later. Using now the flat Friedman–Robertson–Walker metric (as suggested by the Seven-year WMAP data [15]),

$$ds^2 = dt^2 - a(t)^2\left[dx^2 + dy^2 + dz^2\right],$$

and identifying all the background 4-velocities, Einstein's equations reduce to

$$\left(\frac{\dot a}{a}\right)^2 = \frac{8\pi G}{3}\rho_m + \frac{8\pi G}{3}\rho_r + \frac{8\pi G}{3}\rho_c, \tag{4}$$

$$2\frac{\ddot a}{a} + \left(\frac{\dot a}{a}\right)^2 = -8\pi G(p_c + p_r), \tag{5}$$

$$\dot\rho_m + 3\frac{\dot a}{a}\rho_m = 0 \quad \Rightarrow \quad \rho_m = \rho_{m0}/a^3, \tag{6}$$

$$\dot\rho_r + 4\frac{\dot a}{a}\rho_r = 0 \quad \Rightarrow \quad \rho_r = \rho_{r0}/a^4, \tag{7}$$

$$\dot\rho_c + 3\frac{\dot a}{a}(\rho_c + p_c) = 0 \quad \left(p_c = B\rho_c - A/\rho_c^\alpha\right)$$

$$\Rightarrow \quad \rho_c = \left\{A_s + \frac{1 - A_s}{a^{3(1+\alpha)(1+B)}}\right\}^{1/(1+\alpha)}. \tag{8}$$

In the above set of equations we have defined $A_s = \frac{A}{(1+B)\rho_{c0}^{1+\alpha}}$.

The perturbed equations in the synchronous coordinate condition can be established following closely the computation shown in Ref. [7]. We introduce fluctuations around the background quantities, $g_{\mu\nu} = \bar g_{\mu\nu} + h_{\mu\nu}$, $\rho = \bar\rho + \delta\rho$, $p = \bar p + \delta p$, $u^\mu = \bar u^\mu + \delta u^\mu$. The bars indicate the background quantities. The synchronous coordinate condition implies $h_{\mu 0} = 0$ and $\delta u^0 = 0$. The final perturbed equations read (see also [16]),

$$\frac{\ddot h}{2} + \frac{\dot a}{a}\dot h - 4\pi G(\delta\rho + 3\delta p) = 0, \tag{9}$$

$$\dot\delta\rho + \frac{3\dot a}{a}(\delta\rho + \delta p) + (\rho + p)\left(\theta - \frac{\dot h}{2}\right) = 0, \tag{10}$$

$$(p + \rho)\dot\theta + \left[(\dot\rho + \dot p) + \frac{5\dot a}{a}(\rho + p)\right]\theta + \frac{\nabla^2\delta p}{a^2} = 0, \tag{11}$$

where ρ and p stand for the total matter and pressure, respectively, $\theta = \delta u^i_{\ i}$ and $h = h_{kk}/a^2$.

In terms of the components, we end up with the following equations:

$$\frac{\ddot h}{2} + \frac{\dot a}{a}\dot h - 4\pi G\left[\delta\rho_m + \delta\rho_c + \delta\rho_r + 3(\delta p_m + \delta p_c + \delta p_r)\right] = 0, \tag{12}$$

$$\delta\dot\rho_m + \frac{3\dot a}{a}(\delta\rho_m + \delta p_m) + (\rho_m + p_m)\left(\theta_m - \frac{\dot h}{2}\right) = 0, \tag{13}$$

$$(\rho_m + p_m)\dot\theta_m + \left[(\dot\rho_m + \dot p_m) + \frac{5\dot a}{a}(\rho_m + p_m)\right]\theta_m + \frac{\nabla^2\delta p_m}{a^2} = 0, \tag{14}$$

$$\delta\dot\rho_c + \frac{3\dot a}{a}(\delta\rho_c + \delta p_c) + (\rho_c + p_c)\left(\theta_c - \frac{\dot h}{2}\right) = 0, \tag{15}$$

$$(\rho_c + p_c)\dot\theta_c + \left[(\dot\rho_c + \dot p_c) + \frac{5\dot a}{a}(\rho_c + p_c)\right]\theta_c + \frac{\nabla^2\delta p_c}{a^2} = 0, \tag{16}$$

$$\delta\dot\rho_r + \frac{3\dot a}{a}(\delta\rho_r + \delta p_r) + (\rho_r + p_r)\left(\theta_r - \frac{\dot h}{2}\right) = 0, \tag{17}$$

$$(\rho_r + p_r)\dot\theta_r + \left[(\dot\rho_r + \dot p_r) + \frac{5\dot a}{a}(\rho_r + p_r)\right]\theta_r + \frac{\nabla^2\delta p_r}{a^2} = 0, \tag{18}$$

with $\theta_m = \delta u^i_{m,i}$, $\theta_c = \delta u^i_{c,i}$ and $\theta_r = \delta u^i_{r,i}$.

With the definitions

$$\Omega_c(a) = \Omega_{c0}\left(A_s + \frac{1 - A_s}{a^{3(1+\alpha)(1+B)}}\right)^{\frac{1}{1+\alpha}}, \tag{19}$$

$$w(a) = \frac{p_c}{\rho_c} = B - \frac{A_s(1 + B)}{A_s + (1 - A_s)a^{-3(1+\alpha)(1+B)}}, \tag{20}$$

$$v_s^2(a) = B + \frac{\alpha A_s(1 + B)}{A_s + (1 - A_s)a^{-3(1+\alpha)(1+B)}}, \tag{21}$$

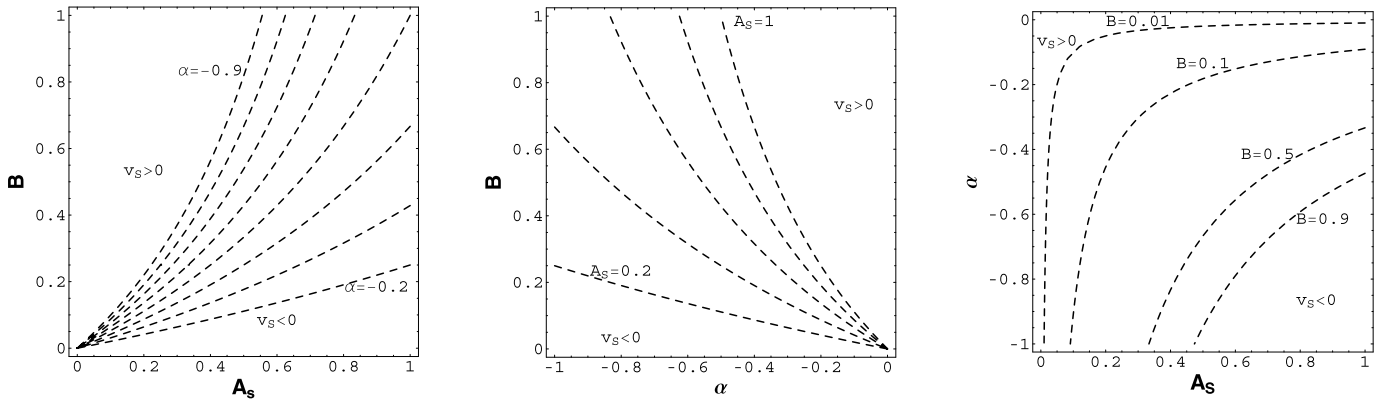

Fig. 1. In each panel we have fixed one of the parameters (α, A_s, B) and plotted the contours for which the speed of sound is equal to zero. Above (below) each dashed line we have $v_s^2 > 0$ ($v_s^2 < 0$) for different values of α–(A_s)–(B) in the left–(center)–(right) panel.

$$H(a) = \left(\frac{\Omega_{m0}}{a^3} + \Omega_c(a) + \frac{\Omega_{r0}}{a^4}\right)^{1/2}, \tag{22}$$

$$q(a) = \frac{\frac{\Omega_{m0}}{a^3} + \Omega_c(a)(1+3w(a)) + \frac{2\Omega_{r0}}{a^4}}{2(\frac{\Omega_{m0}}{a^3} + \Omega_c(a) + \frac{\Omega_{r0}}{a^4})} \tag{23}$$

and remembering that $p_m = \delta p_m = 0$, leading also to $\theta_m = 0$ up to an irrelevant non-homogeneous term, the set equations becomes

$$\delta'' + \big[2 - q(a)\big]\frac{\delta'}{a} - \frac{3\Omega_{m0}}{2a^5[H(a)]^2}\delta = \frac{3\Omega_c(a)}{2[aH(a)]^2}\lambda\big[1 + 3v_s^2(a)\big] + \frac{3\Omega_{r0}}{a^6[H(a)]^2}\delta_r, \tag{24}$$

$$\lambda' + \frac{3}{a}\big[v_s(a) - w(a)\big]\lambda = -\big[1 + w(a)\big]\left[\frac{\theta_c(a)}{aH(a)} - \delta'\right], \tag{25}$$

$$\big[1 + w(a)\big]\left\{\theta_c' + \frac{[2 - 3v_s^2(a)]}{a}\theta_c\right\} = v_s^2(a)\left(\frac{k}{k_0}\right)^2\frac{\lambda}{H(a)a^3}, \tag{26}$$

$$\delta_r' + \frac{4}{3}\left(\frac{\theta_r}{aH(a)} - \delta'\right) = 0, \tag{27}$$

$$\theta_r' + \frac{\theta_r(a)}{a} = \left(\frac{k}{k_0}\right)^2\frac{\delta_r}{4H(a)a^3}, \tag{28}$$

where

$$\delta \equiv \frac{\delta\rho_m}{\rho_m}, \qquad \lambda \equiv \frac{\delta\rho_c}{\rho_c}, \qquad \delta_r \equiv \frac{\delta\rho_r}{\rho_r} \tag{29}$$

and $k_0^{-1} = 3000$ h Mpc. A Fourier decomposition of the spatial dependence of the perturbed quantities has been performed, k being the corresponding Fourier mode. Remark that $1 + w(a) > 0$ since $w(a) > -1$ always for the present epoch, approaching $w(a) = -1$ only asymptotically in the future.

3. Numerical analysis

The matter power spectrum is defined by

$$\mathcal{P} = \delta_k^2, \tag{30}$$

where δ_k is the Fourier transform of the dimensionless density contrast δ. In what follows we will use the matter power spectrum data of the 2dFGRS observational mapping [17]. We use the data in the range 0.01 Mpc^{-1} h $< k <$ 0.185 Mpc^{-1} h (here h is connected with the Hubble parameter today being defined by $H_0 = 100$ h km/(Mpc s), with no relation to the previous definition of the metric fluctuation) which corresponds to the linear regime which is being considered here. Hence, the covariance matrix is diagonal.

One important aspect of the numerical analysis is to fix the initial conditions. In order to do so, we use a scale invariant primordial spectrum, with the BBKS transfer function [18]. The initial conditions are fixed following in general lines the prescription described in reference [19]. Since the initial condition may be fixed at $z \gtrsim 1000$, when essentially radiation is still strongly coupled to matter, the initial conditions for the radiative fluid are the same as for the pressureless component. The results, however, are the same if we ignore the radiative fluid and impose the initial conditions at $z < 1000$. Even if a full statistical analysis may be performed using, for example, the Bayesian method, such complete analysis is not essential to obtain the main result of this work.

In any perturbative analysis, one crucial quantity is the squared sound speed. Positive values are assured if B and α are positive, see Eq. (21). It is possible to have also positive squared speed in the case α is negative, but in a very small range. The possibility to have $v_s^2 > 0$ and $B < 0$ is almost excluded, as it can be seen in Fig. 1. However, in performing the numerical computation we will consider this possibility.

In the usual ΛCDM model there are two pressureless components: the baryons and dark matter. The Modified Chaplygin Gas model we are studying here is intended to be a unification model, where the dark sector is covered by a unique exotic fluid, with pressure given by (1). This is the so-called quartessence model. In this case, the pressureless component is given just by baryons, and we can fix (having in mind the CMB and nucleosynthesis results) $\Omega_{m0} = 0.043$. It is possible also to include, besides the modified Chaplygin gas fluid, an extra dark matter component. In doing so, we do not have in mind a unification scenario, and the model is called quintessence model. This possibility will be also explored.

The power spectrum will be computed for the pressureless component. Actually, the power spectrum provides information about the matter clustering at $z = 0$, when the Modified Chaplygin Gas behaves as dark energy, and consequently, giving no (direct) contribution to $\mathcal{P}_k$ or δ_k^2. At $z = 0$, its effects are indirectly inferred on the distribution of baryonic matter. Also, it is expected that the Modified Chaplygin Gas model may cluster locally, giving rise to a dark matter-like behavior at small scales. Such clustering of the dark energy component must occur only when perturbations reach the non-linear regime. Since, we are interested in large scale perturbations, at linear level, it is not necessary to take into account such contribution for the computation of the power spectrum.

In Fig. 2 we plot the linear matter power spectrum for the quartessence model comparing with the observational data for $A_s = 0.95$ and $\alpha = 10$ (left panel) and $\alpha = 1$ (right panel), with dif-

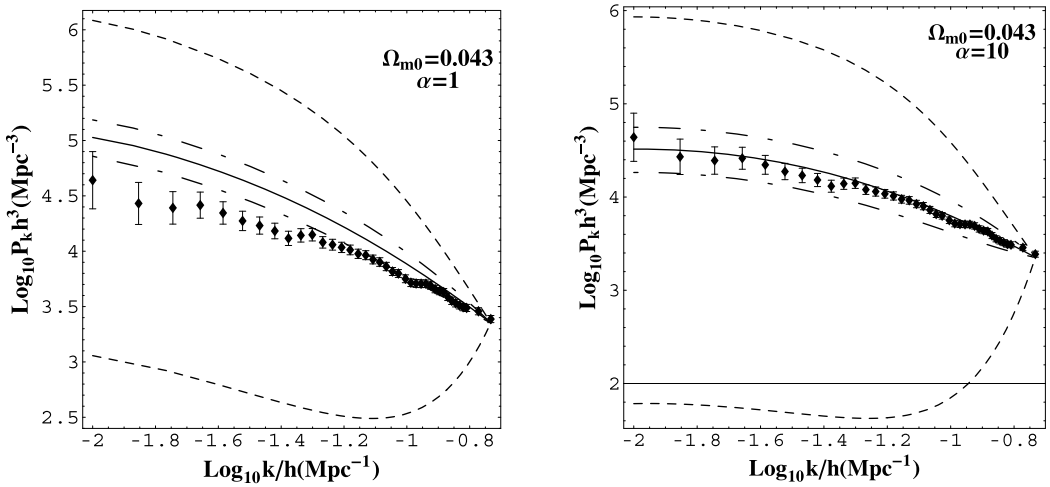

Fig. 2. At left, power spectrum for the quartessence MCG model ($\Omega_{m0} = 0.043$) fixing $A_s = 0.95$ and $\alpha = 1$. From top to bottom, the curves are MCG models with $B = 10^{-4}$, $B = 10^{-5}$, $B = 0$, $B = -10^{-5}$ and $B = -10^{-4}$, respectively. At right, power spectrum for $\alpha = 10$, and for the same values as before of the parameters A_s and B.

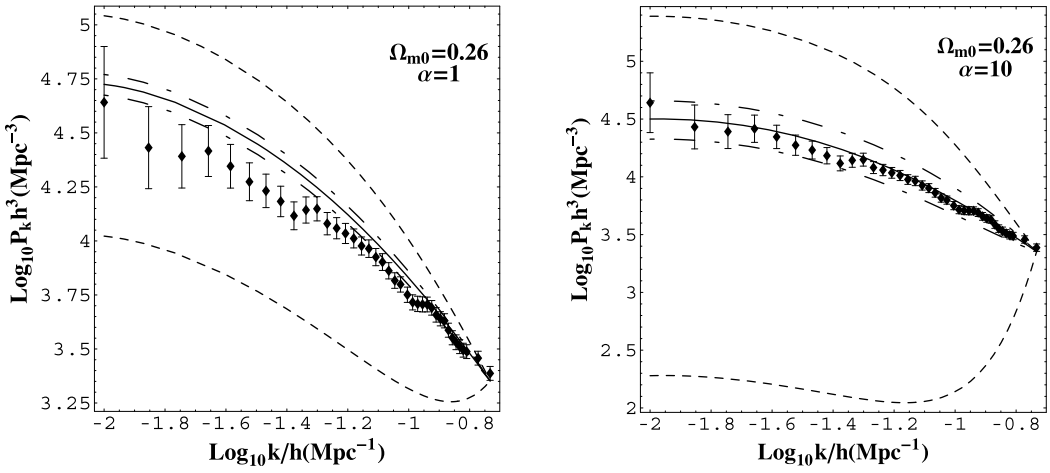

Fig. 3. At left, power spectrum for the quintessence MCG model ($\Omega_{m0} = 0.26$) fixing $A_s = 0.95$ and $\alpha = 1$. From top to bottom, the curves are MCG models with $B = 10^{-4}$, $B = 10^{-5}$, $B = 0$, $B = -10^{-5}$ and $B = -10^{-4}$, respectively. At right, power spectrum for $\alpha = 10$, and for the same values as before of the parameters A_s and B.

ferent values of B. When $\alpha = 10$, the case $B = 0$ is essentially the only one that fits the observational data, with a total χ^2 of about 17 (the statistical parameter that measure, to say in general lines, the quality of the fitting of the data by a theoretical model, the smaller the value of χ^2 the better the fitting). As it can be verified, when $|B| > 10^{-4}$ there is already a huge discrepancy between the theoretical results and the observational data. At the right panel of the same figure, the only changing is $\alpha = 1$. Now the better fitting is achieved by $B = -2.7 \times 10^{-4}$, but with $\chi^2 \sim 37$: the fitting is much worse than in preceding case. An extensive inspection of the different possibilities shows that a reasonable agreement can be find only around $|B| < 10^{-6}$, with $\alpha \gg 1$ or $\alpha \approx 0$. Such fine tuning in the EoS parameter (1) implies that the only "natural" value would be $B = 0$. This reduces the model to the GCG model. Hence, the confrontation with the matter power spectrum data seems to rule out the MCG model. The same scenario emerges when a quintessence model, with $\Omega_{m0} = 0.26$ is implemented, see Fig. 3.

4. Conclusions

The Modified Chaplygin Gas (MCG) model is an extension of the Generalized Chaplygin Gas (GCG) model, with the addition of a new term in the usual GCG equation of state which is proportional to the density. In this sense, it can be seen as a combination of the CGM model (where $p = -A/\rho_c^{\alpha}$) and the so-called XCDM model (where $p = B\rho$). In the present Letter we have confronted the MCG model against the power spectrum observational data. In general, the MCG leads to good behavior concerning the background tests. However, the power spectrum analysis implies to perform a perturbative study of the model, testing in this sense the deep content of the theoretical framework. In this perturbative analysis, a crucial quantity is the squared sound speed which must be positive in order to avoid instabilities. In the MCG model, the positivity of the squared sound speed requires B and α to be also positive, even if small range of negative values of B and α can in principle be admitted.

However, the confrontation of the MCG model with the power spectrum observational data rules out any significant departures from $B = 0$. In fact, only values such that $|B| < 10^{-6}$ the model can fit the observational data. This result essentially rule out the MCG model, reducing it to the GCG model. Crossing these results with those of reference [6,7], where power spectrum constraints on the GCG model were establisheds, only the quartessence version of the GCG model survives. In the quartessence formulation of the GCG model, the matter content is given only by the baryonic component. If this quantity is left free, we find a prediction of a universe dominated only by matter, in contradiction to the supernova analysis [5].

It must be remarked however that the conclusions obtained in the present work are restricted to a hydrodynamical representation of the dark energy component. If this component is alternatively represented by a self-interacting scalar field, leading to the same background relations, the restrictions arising from the positivity of the squared sound speed disappears. If the MCG model can survive the observational tests in this alternative formulation is a question we intend to address in a future work. The main difficult comes from the fact that the usual GCG gas is connected a kind of Born-Infeld, which leads to essentially the same expression for the sound speed as in the hydrodynamical formulation [20]. Hence the restrictions found here for the hydrodynamical formulation may remain. If such problem can be circumvented in the case MCG model is an open question.

Acknowledgements

J.C.F. and H.E.S.V. thank CNPq (Brazil) and FAPES (Brazil) for partial financial support. C.O. and J.T. thank the Africa–Brazil scientific cooperation program *Pró-África-CNPq* for partial financial support, and the Departamento de Física of UFES for the kind hospitality during part of the elaboration of this work.

References

[1] R.R. Caldwell, M. Kamionkowski, Ann. Rev. Nucl. Part. Sci. 59 (2009) 397.
[2] A.Y. Kamenshchik, U. Moschella, V. Pasquier, Phys. Lett. B 511 (2001) 265.
[3] M.C. Bento, O. Bertolami, A.A. Sen, Phys. Rev. D 66 (2002) 043507.
[4] R. Jackiw, A particle field theorist's lectures on supersymmetric, non-abelian fluid mechanics and d-branes, physics/0010042.
[5] R. Colistete Jr, J.C. Fabris, S.V.B. Gonçalves, P.E. de Souza, Int. J. Modern Phys. D 13 (2004) 669;
R. Colistete Jr., J.C. Fabris, S.V.B. Gonçalves, Int. J. Modern Phys. D 14 (2005) 775;
R. Colistete Jr., J.C. Fabris, Class. Quantum Grav. 22 (2005) 2813.
[6] J.C. Fabris, S.V.B. Gonçalves, H.E.S. Velten, W. Zimdahl, Phys. Rev. D 78 (2008) 103523.
[7] J.C. Fabris, H.E.S. Velten, W. Zimdahl, Phys. Rev. D 81 (2010) 087303.
[8] Y. Wu, S. Li, J. Lu, X. Yang, Mod. Phys. Lett. A 22 (2007) 783.
[9] J. He, Y.-B. Wu, F.-H. Fu, Chinese Phys. Lett. 25 (1978) 347.
[10] M.L. Bedran, V. Soares, M.E. Araujo, Phys. Lett. B 659 (2008) 462.
[11] J. Lu, L. Xu, J. Li, B. Chang, Y. Gui, H. Liu, Phys. Lett. B 662 (2008) 87.
[12] D.-J. Liu, X.-Z. Li, Chinese Phys. Lett. 22 (2005) 1600.
[13] U. Debnath, S. Chakraborty, Int. J. Theor. Phys. 47 (2008) 2663.
[14] S. Costa, M. Ujevic, A.F. dos Santos, Gen. Relativ. Gravitat. 40 (2008) 1683.
[15] E. Komatsu, et al., Seven-year Wilkinson microwave anisotropy probe (WMAP) observations: cosmological interpretation, arXiv:1001.4538.
[16] S. Weinberg, Gravitation and Cosmology, Wiley, New York, 1972.
[17] S. Coles, et al., MNRAS 362 (2005) 505.
[18] J.M. Bardeen, J.R. Bond, N. Kaiser, A.S. Szalay, Astrophys. J. 304 (1986) 15.
[19] J.C. Fabris, I.L. Shapiro, J. Solà, JCAP 0702 (2007) 016.
[20] C.E.M. Batista, J.C. Fabris, M. Morita, Gen. Relativ. Gravitat. 42 (2010) 839.